EUROPEAN ORGANIZATION FOR NUCLEAR RESEARCH

CERN-EP/86-96
25 July 1986

MEASUREMENT OF THE 4f STRONG INTERACTION LEVEL WIDTH IN LIGHT ANTIPROTONIC ATOMS

D. Rohmann, H. Barth, A.D. Hancock*), H. Koch, Th. Köhler, A. Kreissl**), H. Poth, U. Raich**) and A. Wolf**)

Kernforschungszentrum Karlsruhe, Institut für Kernphysik and Universität Karlsruhe, Institut für Experimentelle Kernphysik, Fed. Rep. Germany

L. Tauscher

Institute for Physics, University of Basle, Switzerland

M. Suffert

Centre de Recherches Nucléaires, Strasbourg, France

M. Chardalas and S. Dedoussis

Department of Nuclear Physics, University of Thessaloniki, Greece

A. Nilsson

Research Institute of Physics, Stockholm, Sweden

W. Kanert, T. von Egidy, F.J. Hartmann and G. Schmidt

Physik Department der Technischen Universität, Munich, Fed. Rep. Germany

J.J. Reidy

Physics Department, University of Mississippi, University, Miss., USA

ABSTRACT

The yields of the atomic 4→3 transitions in antiprotonic ^{14}N, $^{16,17,18}O$, ^{19}F, and ^{23}Na were measured at the CERN antiproton facility, LEAR. From these, the widths Γ_{up} of the 4f levels were determined to be 136 ± 19 meV (^{14}N); 603 ± 22 meV (^{16}O); 731 ± 35 meV (^{17}O); 795 ± 23 meV (^{18}O); 2.79 ± 0.16 eV (^{19}F); and 23.8 ± 7.4 eV (^{23}Na).

(Submitted to Zeitschrift für Physik A)

---

*) Present address: EG&G, Los Alamos, New Mexico, USA.
**) At present CERN, Geneva, Switzerland.

1. INTRODUCTION

Exotic atoms are appropriate systems for the study of the strong-interaction potential between the antiproton and the nucleus at very low energies. The influence of the strong interaction shows up as a shift ε (difference between the measured energy and the calculated electromagnetic energy, $\varepsilon = E_{exp} - E_{em}$) of the atomic transition energies and as a broadening Γ of the atomic levels, measured by the line position and the line shape, respectively. Moreover, the absorption of the antiproton by the nucleus attenuates the atomic X-ray transitions. The shift and the width (Γ_{low}) of the lower level can be directly evaluated from the last observable atomic X-ray transition. The width (Γ_{up}) of the next higher level can be deduced from the intensity balance [1]. We have reported on our results for the (lower) 3d level (ε, Γ_{low}) of antiprotonic $^{16,17,18}O$ in an earlier publication [2]. Here we report on the systematic study of the widths of the (upper) 4f level (Γ_{up}) for the antiprotonic ^{14}N, $^{16,17,18}O$, ^{19}F, and ^{23}Na atoms.

2. EXPERIMENT

The experimental technique has already been described in some detail (ref. [2] and references therein). Here we will give only a short summary.

We measured the $\bar{p}$-atomic X-rays for several nuclei whose last observable atomic transition is the 4→3 at the M1 beam of the low-energy antiproton ring (LEAR) at CERN. The incident $\bar{p}$ momenta were 300 MeV/c or 200 MeV/c. Sandwiched between two scintillation counters in coincidence, a polyethylene moderator slowed down the $\bar{p}$'s to be stopped in the target. We used a sodium fluoride crystal for the measurement on ^{19}F and ^{23}Na (5 spills ≡ 647 x 10^6 stopped $\bar{p}$); water in an aluminium frame with Be foils glued to it, for the oxygen isotopes ^{16}O (4 spills ≡ 296 x 10^6 stopped $\bar{p}$), ^{17}O (11 spills ≡ 817 x 10^6 stopped $\bar{p}$) and ^{18}O (9 spills ≡ 568 x 10^6 stopped $\bar{p}$); and the contribution from stops in air (target $^{6,7}Li$) for ^{14}N (4 spills ≡ 680 x 10^6 stopped $\bar{p}$). The FWHM of the range curves was of the order of 50 to 150 mg/cm^2, and thus smaller than the target thickness of 300 mg/cm^2. The average $\bar{p}$ stop-rate was about 27 x 10^3 s^{-1} (15 x 10^3 s^{-1}) for 300 MeV/c (200 MeV/c) $\bar{p}$ beam momentum. The X-rays were registered by four to six solid-state [Ge and Ge(Li)] detectors of various dimensions and energy ranges. The time of arrival and the energy of each event were stored on line in two-dimensional arrays in a MC68000 microprocessor memory. These arrays as well as the projected energy and time spectra were transferred to a PDP 11/34 computer for further data handling and evaluation.

3. DATA EVALUATION AND RESULTS

The energy calibration, energy resolution, and relative efficiency of each detector were determined off line with radioactive sources and counter-checked with those $\bar{p}$-atomic X-ray lines which are not disturbed by strong-interaction effects. The detection efficiency as a function of energy was determined by fitting a semi-empirical formula for Ge(Li) detectors (eq. (8) in ref. [3]) to the experimental data (fig. 1). The shapes of the efficiency curves determined off beam were controlled under beam conditions and proved not to change under beam load.

The spectra around the 4→3 region obtained with one of the detectors are shown in fig. 2. The lines were fitted using standard procedures [2].

For each detector the measured intensities of the $\bar{p}$ lines were corrected for efficiency and for target absorption. Table 1 shows the error-weighted means (all detectors) of the corrected intensities, normalized to the 5→4 intensity.

The yield Y of the last X-ray transition (in this case 4→3) is given by

$$Y(4\to3) = P(4f)\,\frac{\Gamma_{rad}}{\Gamma_{up} + \Gamma_{rad} + \Gamma_{Aug}}\,, \qquad (1)$$

where Γ_{rad}, Γ_{Aug}, and Γ_{up} are the radiation, the Auger, and the strong-interaction widths of the 4f level, respectively, and P(4f) is its population. If this level is fed only by X-ray transitions its population can be determined from the intensities I of these X-rays:

$$P(4f) = \sum_{n\geq5} I(n\to4)\,. \qquad (2)$$

Thus an upper width can be derived from the measured intensities by

$$\Gamma^{*}_{up} = \Gamma_{rad}\left(\frac{\sum_{n\geq5} I(n\to4)}{I(4\to3)} - 1\right) - \Gamma_{Aug}\,. \qquad (3)$$

The results of eq. (3) using the measured X-ray intensities are also given in table 1; Γ_{rad} and Γ_{Aug} were taken from refs. [4] and [5]. The errors are purely statistical.

The assumption of eq. (2) has to be verified for the following reasons:

a) The transitions n→4 have not been measured up to the series limit.

b) The measured intensities may still contain unresolved parallel transitions of the type (n, l=3) → (4, l=2), etc.

c) Radiationless Auger transitions may feed the 4f level.

Points (a) and (c) lead to an underestimate of P(4f) from eq. (2), whereas point (b) leads to an overestimate. In order to resolve these problems, we have to compare the measured intensity values with cascade calculations. For this we

use a code based on a cascade program written by Hüfner [5], and described in more detail in ref. [6]. The intensities of the X-ray transitions are calculated by starting the atomic cascade at n = 40 and assuming a modified initial statistical population of the form $P_{40,l} = (2l + 1)e^{\alpha l}$, the $P_{40,l}$ normalized such that $\sum_l P_{40,l} = 1$. For the gas ^{14}N we took into account that there are only 5 L electrons for a refilling of the electron K shell once a K electron has been kicked out.

In addition to what was described in ref. [6], the $\bar{p}$ absorption was included in the code. The experimental strong-interaction widths Γ_{low} of the lower level (see ref. [2]) and the initial values $\Gamma^0_{up} = \Gamma^*_{up}$ for the upper levels are given as input parameters (Γ^0_{up} is a fit parameter). The strong interaction widths for the higher levels in the cascade are scaled from these values. This scaling is based on the overlap of the particle ($\bar{p}$) Coulomb wave function with the nucleus, represented by a uniform distribution of radius $R = r_0 A^{1/3}$, $r_0 = 1.2$ fm. The absorption widths of circular orbits $\Gamma_{n',l'=n'-1}$ are computed according to

$$\Gamma_{n',l'=n'-1} = \Gamma_{n,l=n-1} \frac{(2l + 3)!\ (l + 1)^{2l+3}}{(2l' + 3)!\ (l' + 1)^{2l'+3}} \left(\frac{2ZR}{a_{\bar{p}}}\right)^{2(l'-l)} (l' + 1)^2 \quad (4)$$

[where $a_{\bar{p}} = \hbar^2/(m_{\bar{p}}e^2)$], starting with $\Gamma_{l+1,l} = \Gamma^0_{up}$. Since such a geometrical scaling is only a crude approximation, the factor $(l' + 1)^2$ in eq. (4) was arbitrarily chosen so as to reproduce the measured intensities better. It corresponds to an effective softer decrease of the absorption widths with l.

The scaling for the absorption widths with increasing n and fixed l was given by West [7]. We use a refined version, based again on the overlap scaling described above:

$$\Gamma_{n',l} = \Gamma_{n,l} \frac{(n' + n - 1)!}{(2n - 1)!\ (n' - n)!} \left(\frac{n}{n'}\right)^{2l+4}, \quad (5)$$

where $\Gamma_{n,l}$ are the widths of the circular orbits calculated from eq. (4).

Using this cascade model we first varied α for a fixed Γ^0_{up}; then, keeping α fixed at the value thus found, we varied Γ^0_{up}. For the best fit we derived the quantity Γ_{up} defined by

$$\Gamma_{up} = \Gamma_{rad}\left(\left[\frac{P(4f)}{I(5\to4)}\right]_{cas} \times \frac{1}{I_{exp}(4\to3)} - 1\right) - \Gamma_{Aug}. \quad (6)$$

The essential difference compared to eq. (3) is that now the population of the 4f level is calculated on the basis of the cascade model adjusted to reproduce the experimental intensities. The results for Γ_{up} are given in table 1. The errors

given there are the square roots of the quadratic sums of the changes in Γ_{up} from α of the best fit to $\alpha' = \alpha \pm 0.01$, of the error arising from a similar treatment for Γ^0_{up} [$\Gamma^{0\,\prime}_{up} = \Gamma^0_{up} \pm 10$ meV (100 meV for ^{23}Na)], and of our experimental error. The first one is of the order of 10-15 meV (135 meV for ^{23}Na), the second of the order of 1 meV (7 meV for ^{23}Na). Thus the leading contribution of the derived errors for Γ_{up} is due to statistics.

The values for Γ^*_{up} and Γ_{up} agree quite well, indicating that the assumption of eq. (2) was justified within the accuracy of the experiment.

4. DISCUSSION

Figure 3 shows the strong-interaction widths Γ_{up} for the $\bar{p}$-atomic 4f level as a function of the atomic weight for the various $\bar{p}$ atoms together with the results from our earlier measurement [8].

Our new values for ^{14}N, ^{16}O, and ^{18}O agree very well with the earlier ones, the errors being considerably smaller. The 4f width increases by 27% $\pm$ 2% from ^{16}O to ^{18}O, which is close to the isotope effect observed in the 3d level [2].

The data exhibit a clear A dependence, which is essentially described by the overlap of the $\bar{p}$-Coulomb wave function with the nucleus [$\Gamma \sim (ZR)^{2l+3} \sim (ZA^{1/3})^9$]. The isotopes of oxygen clearly show different widths, but also here the effect can be described by the differences in the overlaps. This is demonstrated in fig. 4, where $\Gamma/(ZA^{1/3})^9$ is plotted versus A. The data points seem to be compatible with a constant: $\Gamma/(ZA^{1/3})^9 = (1.054 \pm 0.019) \times 10^{-12}$ [eV]. Hence, the effect in the upper level seems to be rather well handled by a perturbation calculation and justifies *a posteriori* the scaling applied in the cascade calculations eqs. (4) and (5). The influence of the factor $(l' + 1)^2$ in eq. 4 on the determined values for the upper level widths Γ_{up} [eq. (6)] is of the order of 1‰ to 1%.

The width of the 4f level was calculated by several authors in refs. [9] to [12] on the basis of various potential models. Their values are also given in table 1 and fig. 3. Their results reproduce the general trend of our data rather well.

Acknowledgements

We would like to thank the LEAR staff for their collaboration during the data-taking of this experiment. For technical assistance we are grateful to H. Hagn, J. Hauth, E. Hechtl, M. Meyer and P. Stoeckel. We also thank Dr. G. Büche for providing us with the electromagnetic transition energy calculations. The work was supported by the Bundesministerium für Forschung und Technologie of the Federal Republic of Germany, the Swiss National Science Foundation, and the US National Science Foundation.

REFERENCES

[1] H. Koch et al., Phys. Lett. 28B (1968) 279.

[2] Th. Köhler et al., preprint CERN-EP/86-02, to be published in Physics Letters B;
H. Poth et al., 3rd LEAR Workshop on Physics with Antiprotons at LEAR in the ACOL era, Tignes, 1985 (eds. U. Gastaldi, R. Klapisch, J.M. Richard, J. Tran Thanh Van) (Editions Frontières, 1986) p. 581.

[3] F. Hajnal and C. Klusek, Nucl. Instrum. Methods 122 (1974) 559.

[4] E.F. Borie and G.A. Rinker, Rev. Mod. Phys. 54 (1982) 67;
E.F. Borie, Phys. Rev. A28 (1983) 555;
E. Jödicke, KfK-Bericht 3933 (1985).

[5] J. Hüfner, Z. Phys. 195 (1966) 365.

[6] G. Backenstoss et al., Z. Phys. A273 (1975) 137.

[7] D. West, Rep. Prog. Phys. 21 (1958) 271.

[8] H. Poth et al., Nucl. Phys. A294 (1978) 435.

[9] A.M. Green, W. Stepien-Rudzka and S. Wycech, Nucl. Phys. A399 (1983) 307.

[10] T. Suzuki and H. Narumi, Nucl. Phys. A426 (1984) 413.

[11] W.B. Kaufmann and H. Pilkuhn, Phys. Lett. 166B (1986) 279;
W.B. Kaufmann, private communication.

[12] D.A. Sparrow, Phys. Rev. 33C (1986) 287.

Table 1

Experimental and calculated intensities for the n→4 and 4→3 transitions, as well as experimental uncorrected and corrected (see text) widths Γ_{up} for the 4f level for ^{14}N, $^{16\ 17\ 18}O$, ^{19}F, and ^{23}Na

	^{14}N		^{16}O		^{17}O		^{18}O		^{19}F		^{23}Na	
Transition	Exp.	Cas.	Exp.	Cas.	Exp.	Cas.	Exp.	Cas.	Exp.	Cas.	Exp.	Cas.
4→3	35.70(2.60)	35.10	27.13(0.71)	26.21	22.83(0.91)	22.11	20.38(0.42)	20.85	8.31(0.30)	8.11	2.29(0.69)	2.26
5→4	100.00(6.30)	100.00	100.00(1.15)	100.00	100.00(1.05)	100.00	100.00(1.04)	100.00	100.00(2.52)	100.00	100.00(1.81)	100.00
6→4	0.78(1.00)	0.82	24.00(0.33)	24.40	24.50(0.27)	24.59	22.71(0.28)	23.92	10.97(0.23)	12.27	9.14(0.17)	10.00
7→4	0.08(0.10)	0.08	13.01(0.19)	10.79	12.72(0.16)	11.01	12.48(0.15)	10.50	3.55(0.08)	3.49	3.21(0.08)	2.86
8→4		0.02	7.64(0.11)	6.24	7.69(0.08)	6.47	7.51(0.09)	6.04	1.65(0.08)	1.37	1.63(0.09)	1.41
9→4		0.01	4.45(0.09)	4.34	4.45(0.06)	4.55	4.11(0.06)	4.17	0.72(0.05)	0.69	1.06(0.05)	0.98
10→4		0.01	2.71(0.10)	3.20	2.80(0.10)	3.37	2.65(0.08)	3.04	0.61(0.47)	0.39	0.75(0.07)	0.79
11→4		0.01	1.39(0.09)	2.36	1.39(0.08)	2.51	1.42(0.08)	2.22	0.12(0.05)	0.22	0.57(0.07)	0.62
12→4		0.00	0.77(0.08)	1.73	1.04(0.10)	1.88	1.25(0.08)	1.62	0.15(0.03)	0.11	0.31(0.08)	0.42
$\Sigma_n I(n\to4)$	100.86(6.38)	100.95	153.97(1.23)	153.06	154.59(1.11)	154.38	152.13(1.10)	151.51	117.77(2.58)	118.54	116.67(1.83)	117.08
Γ^*_{up} [eV]	0.135(0.018)		0.606(0.021)		0.726(0.034)		0.792(0.022)		2.70(0.16)		23.4(7.4)	
α	+0.58		-0.10		-0.11		-0.10		+0.16		+0.07	
Γ_{rad} [meV]	74.1		129.8		125.9		122.5		204.7		469.3	
Γ_{Aug} [meV]	0.005		0.454		0.435		0.422		0.465		0.501	
Γ_{up} [eV]	0.136(0.019)		0.603(0.022)		0.731(0.035)		0.795(0.023)		2.79(0.16)		23.8(7.4)	
Γ_{up}(theor): [9]			0.47				0.76					
[10]	0.181		0.724				0.893					
[11]	0.14		0.66		0.63		0.84		3.8		22.7	
[12]	0.198		0.87						3.53		23.2	

Figure captions

Fig. 1 : Efficiency curve for one of the X-ray detectors (planar Ge detector with the dimensions 200 mm^2 x 7 mm).

Fig. 2 : X-ray spectra of the light antiprotonic atoms for the 4→3 region.

Fig. 3 : Strong-interaction widths of the $\bar{p}$-atomic 4f level versus the atomic weight of the antiprotonic atoms. △ : ref. [8]. ◇ : ref. [9]. × : ref. [10]. □ : ref. [11]. + : ref. [12]. ● : this experiment.

Fig. 4 : Strong-interaction widths of the $\bar{p}$-atomic 4f level, scaled according to the overlap of the $\bar{p}$ with the nucleus.

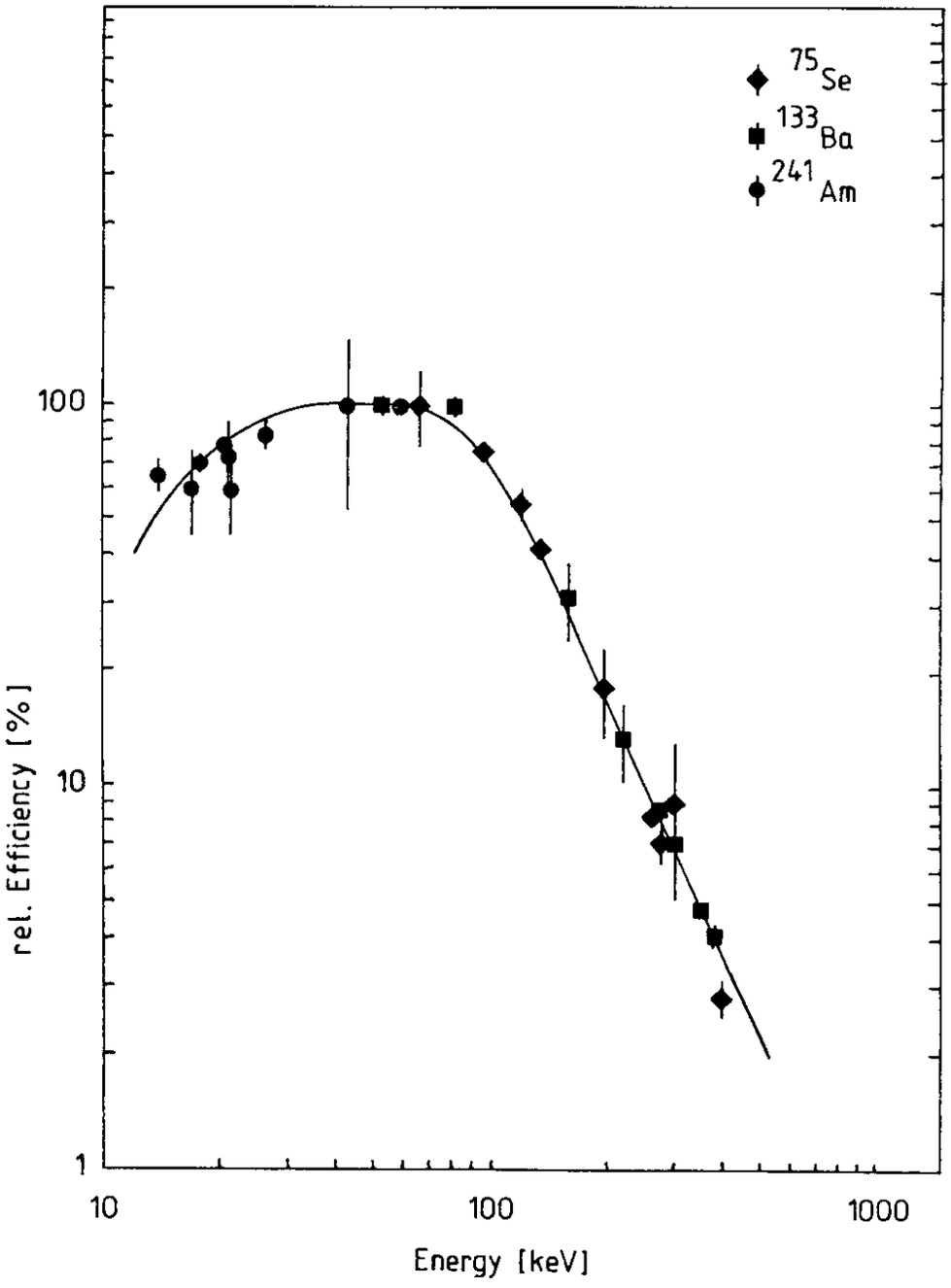
^{75}Se
^{133}Ba
^{241}Am
100
10
1
rel. Efficiency [%]
10
100
1000
Energy [keV]

Fig. 1

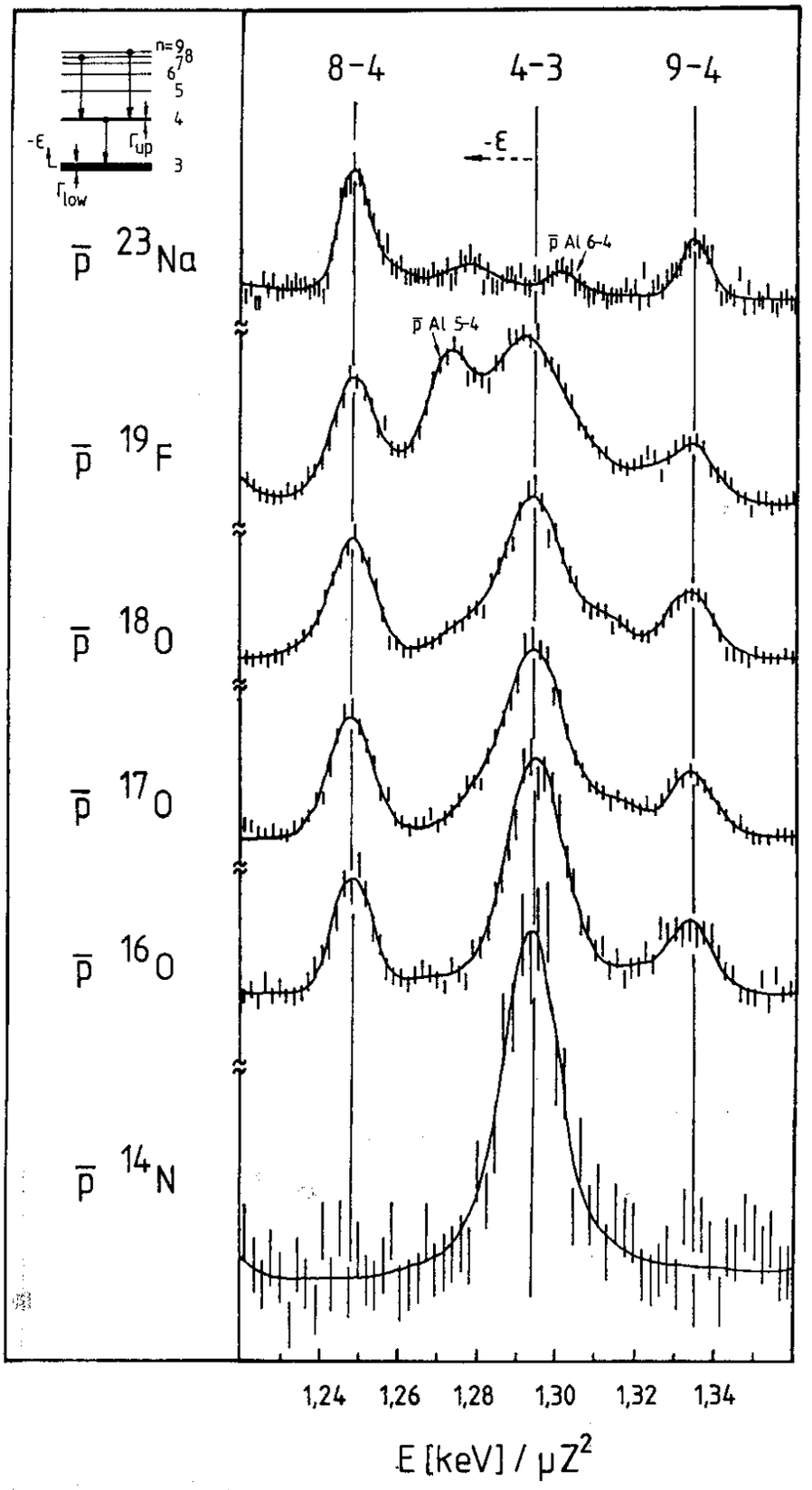
n=9
8
7
6
5
4
3
Γ_{up}
$-\epsilon_L$
Γ_{low}
8-4
4-3
9-4
$-\epsilon$
$\bar{p}$ Al 6-4
$\bar{p}$ Al 5-4
$\bar{p}$ ^{23}Na
$\bar{p}$ ^{19}F
$\bar{p}$ ^{18}O
$\bar{p}$ ^{17}O
$\bar{p}$ ^{16}O
$\bar{p}$ ^{14}N
1,24
1,26
1,28
1,30
1,32
1,34
E [keV] / μZ^2

Fig. 2

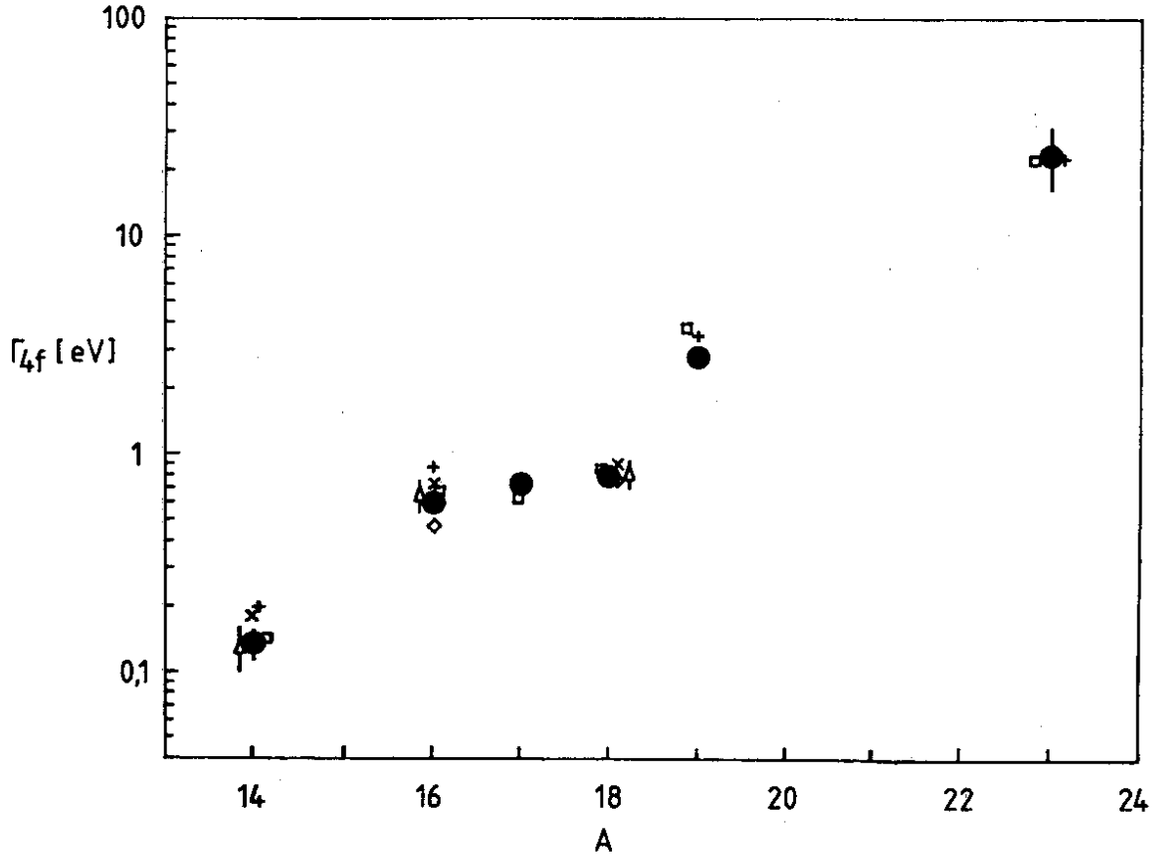
100
10
1
0,1
Γ_{4f} [eV]
14
16
18
20
22
24
A

Fig. 3

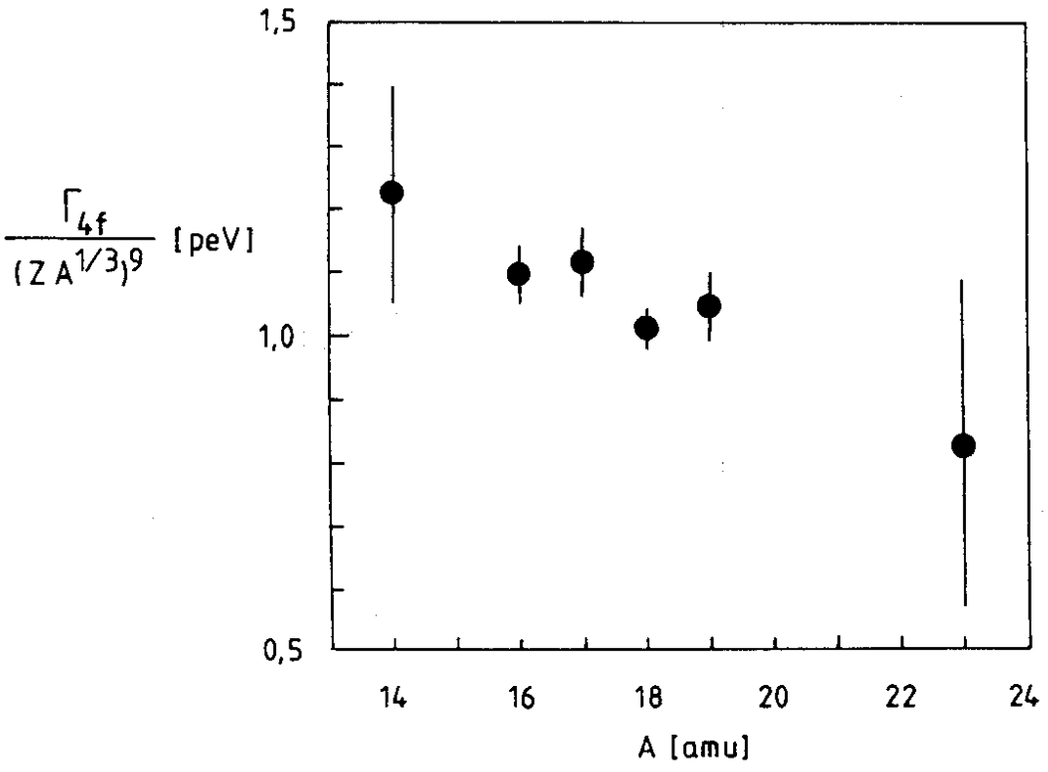
1,5
1,0
0,5
$\frac{\Gamma_{4f}}{(Z\,A^{1/3})^9}$ [peV]
14
16
18
20
22
24
A [amu]

Fig. 4